

Enhanced Energy harvesting, utilizing ZnO nanosheet based nanogenerator embedded in phononic crystal

A. Heydari¹, S. Darbari^{2*}

Received: 2015/10/06 Accepted 2016/1/06

Abstract

In this report, we present a direct current piezoelectric nanogenerator based on ZnO nanosheets, which is driven by ultrasound waves propagating in water. ZnO nanosheets have been grown by hydrothermal method on Al layer as the bottom ohmic contact, while Ni layer serves as the top Schottky contact. Then, we have designed a 1D phononic crystal to realize localized standing wave at the position of nanogenerator, and consequently enhance the energy harvesting performance. The proposed phononic crystal consists of water/steel periodic slabs which are enclosing both sides of the nanogenerator, and the created mid-gap state is matched with the source frequency in the designed structure. Our simulation results confirm that the pressure difference exerted to the nanogenerator is enhanced by a factor of about 12.3, in comparison with the pristine ZnO nanogenerator.

Keywords: phononic crystal, energy harvesting, piezoelectric nanogenerator

Introduction

Energy harvesting is one of the emerging research fields that has attracted many researchers in last few years. Limited amount of fossil resources, air pollutions and increment of energy costs create a significant motivation toward new emerging energy harvesting devices. Piezoelectric nanogenerators (NGs) are one of the candidates for energy harvesting applications. In this line of

research, Wang and colleagues proposed an ultrasound driven piezoelectric NG based on ZnO nanowires, for the first time [1, 2]. Many researchers have worked on ZnO nanowire based NGs to improve their output power, however piezoelectric NGs have always suffer from low power which have confined their application fields significantly. Here, we report an ultrasound driven DC current NG based on ZnO nanosheets, for the first time. ZnO nanosheets benefit from high mechanical stability of the grown networked nanosheets, comparing with ZnO nanorod arrays [3]. Then, we present a NG embedded in 1D phononic crystal (PnC) to improve the energy harvesting performance, for the first time.

Experimental details

As the first step of fabrication process, a 100 nm Al layer is deposited on a pre-cleaned glass substrate. Then, a thin layer of ZnO nanoparticles is coated on the prepared sample, as the seed layer. for this purpose, the sample is immersed in a 0.005 M solution of zinc acetate dehydrate in ethanol, then rinsed by ethanol, and annealed at a temperature of 90°C. This coating procedure is repeated for about three times, to achieve a ZnO seed layer, with a thickness of about 100 nm. The sample is finally annealed for 2 hours, at temperature of 350°C, in order to crystallize the coated seed layer. Then, ZnO nanosheets are synthesized by hydrothermal method. At this step, a hexamethylenetetramine (HMT) ($C_6H_{12}N_4$, 99%), is used as a precursor for the growth of ZnO nanosheets. The concentration of $Zn(NO_3)_2 \cdot 6H_2O$ is 20mM, while the molar ratio of $Zn(NO_3)_2 \cdot 6H_2O$ to HMT is 1:1 [4]. The solution is then transferred into a capped Pyrex vessel in which the pre-coated substrate is floated in the reagent solution, directly beneath the cap. The resulting solution is stirred for 3 hours at a base temperature of about 90°C, by using a magnetic stirrer [4]. The achieved sample is then washed in de-ionized water and air-dried. To complete the structure of nanogenerator, 100 nm Ni layer is deposited on another glass substrate, which can be placed on the nanosheets. Optical image and the prepared SEM image of the synthesized ZnO nanosheets are shown in figure 1.a. It can be observed that lateral dimension of nanosheets are about 3 μm , while the thickness of the sheets is about 50 nm. It is also notable that the

1. ECE Department of Tarbiat Modares University, Tehran, Iran.

2. ECE Department of Tarbiat Modares University, Tehran, Iran. Corresponding author: s.darbari@modares.ac.ir

nanosheets are achieved in a networked structure, which can improve the mechanical stability of the array.

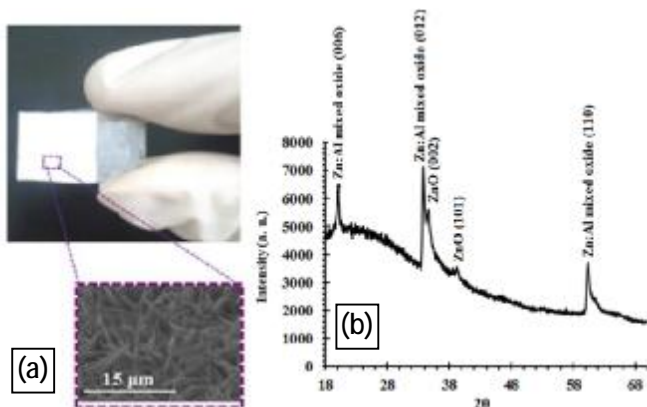


Figure 1. (a) Optical image and SEM image, and (b) XRD result of the grown ZnO nanosheet.

Figure 1.b displays the XRD spectrum of the nanosheets which shows (002), (101) crystalline planes in the grown ZnO sheets. The other observed peaks are related to Zn:Al mixed layer, created at the interface of ZnO/Al layers [3].

Results and discussions

When an external pressure is applied to a ZnO sheet array, the induced stress leads to an internal piezopotential. The compressed side of the piezoelectric nanosheets shows negative polarity, while the stretched side shows positive polarity. Hence, opposing electric currents, induced by the contacting compressed sides of nanosheets can be compensated by the current from stretched sides and no output current can be measured consequently. By choosing a Schottky contact as the top contact, this compensating effect is prevented. Regarding this, and to realize higher mechanical contact area between the top electrode and nanosheets, we have coated Ni on a nano-scale rough substrate and placed this sample on the nanosheet sample to achieve a complete nanosheet/Ni contact. To prepare a nano-scale rough substrate, we have grown an array of short ZnO nanorods with a length of around 300 nm, by hydrothermal method and then completely covered the array by Ni layer. Figure 2.a indicates the fabricated structure schematically, while the insets show the SEM images related to nanorods and nanosheets.

Fig. 2.b and 2.c illustrate the electric

characteristics of the fabricated structure, before and after exerting pressure. Part (a) in this figure exhibits the diode-like behavior relating to the top ZnO/Ni Schottky contact; however due to the height difference between the synthesized nanosheets, there is a weak physical contact between the anode and cathode which can lead to deviation of the achieved electrical behavior from the behavior of an ideal Schottky diode. It can be observed in Fig. 4.b that the pressure induced piezopotential leads to an increment in the measured threshold voltage of the diode. However, the physical contact between the nanosheets and the Ni electrode is realized perfectly in this case, which results in higher measured current.

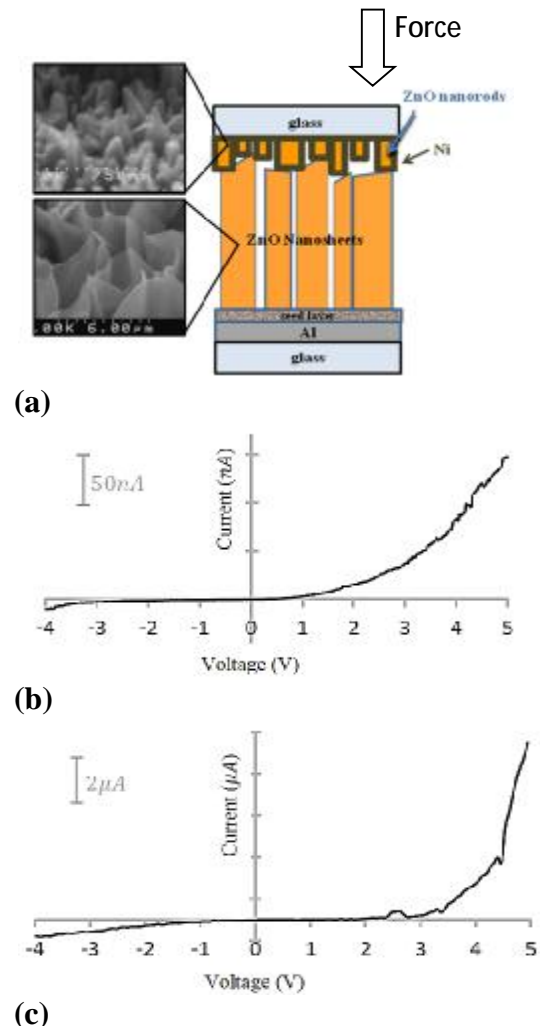
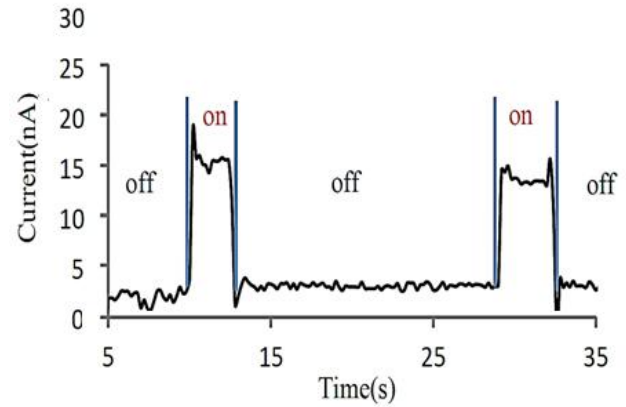
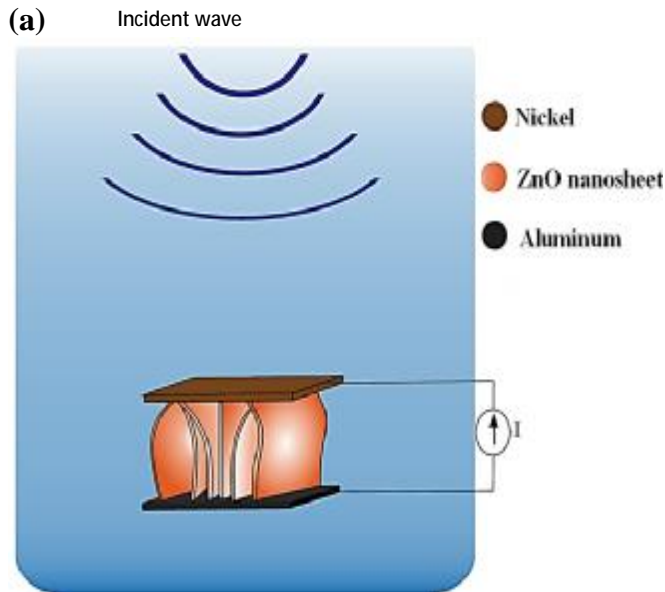


Figure 2. (a) Schematic of the fabricated ZnO nanosheet based NG, utilizing nanorod-based top electrode. I-V characteristics of the fabricated NG: (b) without exerting pressure, and (c) with applying external pressure.

Figure 3.a indicates the fabricated NG which is exposed to ultrasound waves, in water environment. We have chosen water environment

...

[5], because the impedance mismatch ratio between a standard piezoelectric material as ultrasonic source and air is considerably greater than in the case of water. Hence, little power can be transmitted to the exposed NG in the case of air environment. However, water medium is involved with the perfect sealing issues of NG, to avoid to be disturbed by water. Figure 3.b illustrates the measured short circuit current when NG is exposed to on/off states of the driving piezoelectric source. As can be observed, the average value of the measured short circuit direct current is about 15 nA for the fabricated NG. It is observable in the first shot, that the measured I_{sc} shows an overshoot (reaches to about 19 nA) exactly at the instant of starting ultrasound stimulation, but decays to a steady state current (~ 16 nA) after about 1 S. This behavior is observable to some extent, in the second shot of stimulation, and is attributed to transient mechanical response of the device. Also, an acceptable current stability ($\sim 6\%$) and repeatability of about $\pm 10\%$ have been achieved. The distance between the source and NG is about 15 cm, and the actuation frequency of the source is 1.6 MHz, in this experiment.



(b)

Figure 3. (a) Schematic of the ultrasound driven NG and the test setup. (b) The measured short circuit current, when exposed to a couple of on/off cycles of ultrasound wave.

Simulation results of the designed PnC

Phononic crystals are periodic structures made of materials with different elastic properties, which can be arranged in one, two or three dimensions. PnCs prohibit transmitting acoustic/elastic waves with certain frequencies, from the forbidden range for band gap of the crystal. Also, it is well established that existing of a structural defect in the PnC, induces a defect state in the forbidden gap which is depended on the configuration [6]. Existence of a defect state, leads to trap the incident wave with selected frequency around the defect. In other words, selected frequencies can resonate inside the localized PnC based resonator and or the incident energy is confined locally. On the other hand, it is known that electrical output of the piezoelectric NGs is proportional to the exposed pressure field domain. Thus, by designing an appropriate PnC in which our NG plays the role of defect, we can trap and amplify the input mechanical wave around the NG, and can enhance the energy harvesting efficiency.

Considering the operation principle and the force induced by the incident ultrasound wave in Fig. 3.a, we have designed a 1D PnC with periodic slabs parallel to the substrates of our NG, so that the wave vector of the incident waves is perpendicular to the plates of the NG. It is obvious that pressure can be transferred from the incident acoustic plane wave to the nanosheets effectively, in this configuration. Figure 4.a shows the cross section of the ZnO nanosheet based NG, schematically. Since, the length of ZnO

nanosheets is negligible in comparison with the thickness of glass substrates, we have assumed a glassy defect with the thickness of 2 mm, in our simulations. The presented PnC structure consists of periodic slabs of water and steel, to improve the wave coupling from the propagating medium (water), to the PnC. It should be noted that we have applied Finite Element Method (FEM) to solve acoustic/elastic wave equations in our simulations. Fill fraction is defined as $f = a_{steel}/a = 0.5$, Where a_{steel} is thickness of steel layers and a is the period of the PnC. Elastic parameters in the simulations are assumed as presented Table 1. An acoustic plane wave with magnitude of 1Pa, has been assumed as the incident wave.

Table 1. Elastic parameters, applied in the simulations. Wherein ρ , E , ν and c are density, Young modulus, Poisson's ratio and sound speed, respectively

ρ_{steel}	$7850 \frac{\text{kg}}{\text{m}^3}$
ρ_{glass}	$1000 \frac{\text{kg}}{\text{m}^3}$
ρ_{water}	$998 \frac{\text{kg}}{\text{m}^3}$
E_{steel}	$200 \times 10^9 \text{Pa}$
E_{glass}	$50 \times 10^9 \text{Pa}$
ν_{steel}	0.33
ν_{glass}	0.33
c_{water}	$1484 \frac{\text{m}}{\text{s}}$

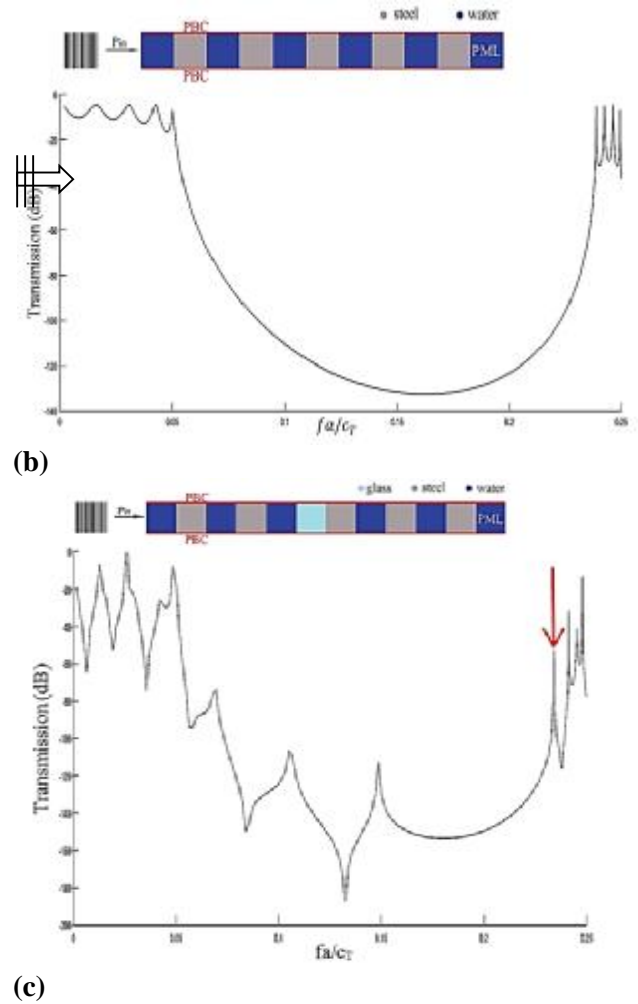
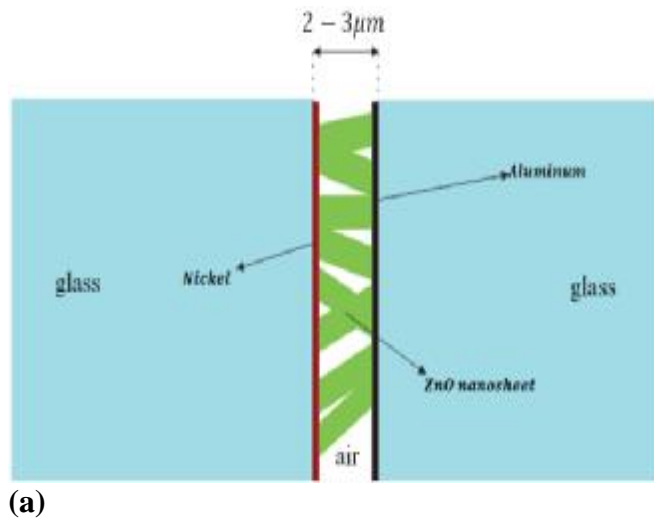


Figure 4. (a) Cross section of the investigated NG. (b) Transmission of the perfect 1D PnC, consisting of steel/water slabs with fill fraction of 0.5. The inset displays the unit cell of the simulated perfect PnC, schematically. (c) Transmission of the defected PnC, in which a glass slab is embedded. The inset shows the related unit cell, which consist of a glass-made defect. Horizontal axes are normalized to fa/c_T .

Figure 4.b depicts the unit cell of the designed perfect 1D PnC schematically, and the relating transmission spectrum which indicates the forbidden gap obviously. The schematic illustrated infinite steel slabs which are immersed and positioned periodically in water environment. It should be noted that the periodicity of the designed 1D PnC is aligned with the incident acoustic wave's propagation. The top and bottom boundary conditions are defined periodic boundary condition (PBC), while the right-end boundary condition is defined perfect matching layer (PML). Horizontal axis in the achieved transmittance spectrum is normalized to fa/c_T ,

Figure 5.a and 5.b illustrate pressure distribution respectively in water slabs and solid slabs (steel and glass), in the defected PnC, at the associated resonant frequency. It can be observed that the pressure difference is enhanced at different sides of embedded NG, comparing with the bare NG. Figure 5.b, also indicates the pressure difference, between two sides of NG at different $\mathbf{fa}/\mathbf{c_T}$ values. As expected, the calculated ΔP value is maximized (≈ 12.3) at the incident frequency which is matched with the defect state (red arrow in Figure 4.c).

Conclusion

References

- [1] Z. Wang, J. Song, “Piezoelectric Nanogenerators Based on Zinc Oxide Nanowire Arrays”, *Science* **312**, 242 (2006).
- [2] X. Wang, “Direct Current Nanogenerator Driven by Ultrasonic Waves”, *Science* **316**, 102 (2007).
- [3] K. H Kim, B. Kumar, K. Y Lee, et al. “Piezoelectric two-dimensional nanosheets/anionic layer heterojunction for efficient direct current power generation”, *Scientific reports* **3** 2017 (2013).
- [4] Y. Zhang, M.K. Ram, E.K. Stefanakos, D. Y. Gosawami,” Synthesis, Characterization, and Applications of ZnO Nanowires”, *Nanomaterials* (2012).
- [5] X. Wang, Y. Gao, Y. Wei, Z. L. Wang, “Output of an Ultrasonic Wave-Driven Nanogenerator in a Confined Tube”, *Nano Res* **2**, 177182 (2009).
- [6] G. Wang et al, “One-dimensional phononic crystals with locally resonant structures”, *Physics Letters A* **327** (2004) 512–521.

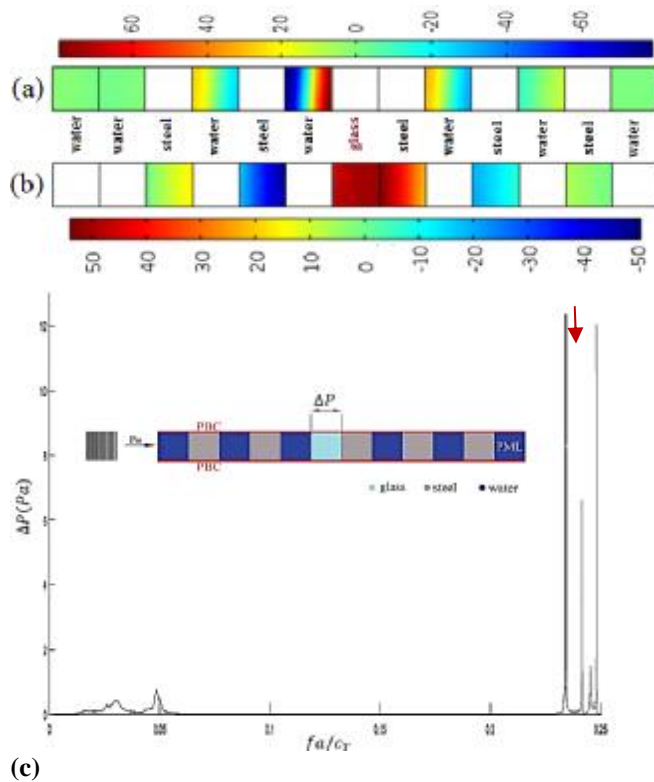


Figure 5. (a) Pressure distribution liquid slabs, and (b) solid slabs, in the defected PnC. (c) Pressure difference between two opposite sides of NG versus fa/c_T , which is maximum at the defect state frequency (red arrow).